

# Effects of Chemical Modification, Tropomyosin, and Myosin Subfragment 1 on the Yield Strength and Critical Concentration of F-Actin<sup>†</sup>

Raffaella Adami,<sup>#</sup> Orietta Cintio,<sup>#</sup> Giorgio Trombetta,<sup>#</sup> Daniel Choquet,<sup>‡</sup> and Enrico Grazi<sup>\*,#</sup>

Dipartimento di Biochimica e Biologia Molecolare, Università di Ferrara, Via Borsari 46, 44100 Ferrara, Italy, and UMR-541 Laboratoire d'Histologie-Embryologie, Université de Bordeaux, France

Received August 16, 2001; Revised Manuscript Received January 30, 2002

**ABSTRACT:** The effects of coupling with tetramethylrhodamine-5-iodoacetamide and of the decoration with tropomyosin and with myosin subfragment 1 on the elastic properties of F-actin filament are investigated. At 22 °C, in 15 mM orthophosphate and 3 mM MgCl<sub>2</sub>, tetramethylrhodamine F-actin displays a yield strength of  $3.69 \pm 0.213$  pN and an elastic modulus by stretching of 0.91 MPa. Decoration with tropomyosin increases the yield strength of tetramethylrhodamine F-actin to  $10.51 \pm 0.24$  pN and the elastic modulus by stretching to 23–75 MPa. Mixtures of myosin subfragment 1 and tetramethylrhodamine F-actin at the 0.2:1, 0.4:1, 0.6:1, 0.8:1, and 1:1 molar ratios are also studied. Both yield strength and the elastic modulus by stretching are found to increase progressively with the ratio. At the 1:1 molar ratio, the yield strength is  $15.81 \pm 0.26$  pN and the elastic modulus by stretching is 13.45 to 40 MPa. Decoration of tetramethylrhodamine F-actin with both tropomyosin and myosin subfragment 1, at the 1:1 molar ratio with the actin monomer, produces filaments with an yield strength of  $22.3 \pm 0.48$  pN.

Yanagida and co-workers were the first to report that the tensile strength of phalloidin decorated F-actin is 200–600 pN (1–3). Since then, it became customary to use these values as a bona fide indication of the tensile strength of the thin filament (4). Actually, tensile strength of natural F-actin is much lower than tensile strength of phalloidin F-actin.

This was shown indirectly by testing the effect of ionic strength on both the critical concentration and tensile strength of phalloidin F-actin. Critical concentration (i.e., the dissociation constant of the elongation reaction) is the main determinant of the free energy of the monomer–monomer interaction, thus of the tensile strength of the actin filament. It was found in fact that the two parameters are inversely related, so that when critical concentration decreases tensile strength increases. At 20 mM ionic strength, critical concentration was ~40 nM and yield strength 34 pN, while at 3 mM ionic strength critical concentration was 146 nM and yield strength was ~6 pN (5).

In an attempt to get ready of rhodamine–phalloidin, which unphysiologically stabilizes the actin filament, tetramethylrhodamine iodoacetamide was coupled directly with F-actin. As a consequence of coupling, about 80% of actin became nonsedimentable. However, the fluorescent nonsedimentable actin was capable of copolymerizing with G-actin yielding fluorescent filaments. The yield strength of these filaments

changes with the ratio of the fluorescent nonsedimentable actin to the G-actin being 1.6, 2.9, and 3.6 pN at the 1/4, 2/3, and 1/1 ratios, respectively. These tensile strengths are approximately 2 orders of magnitude lower than those obtained by decoration of F-actin with phalloidin (6).

We are thus facing a serious problem: how does thin filament in vivo become mechanically competent to skeletal muscle contraction? We have examined here the effects of tropomyosin and of the myosin subfragment 1 on the tensile strength of tetramethylrhodamine F-actin. We have found that both these proteins enhance significantly both the yield strength and the elastic modulus by stretching of the actin filament. Nevertheless, these values are at least 1 order of magnitude lower than is required to support muscle contraction.

## MATERIALS AND METHODS

G-actin (7), myosin (8), and tropomyosin (9) were from rabbit muscle. Heavy meromyosin was obtained by chymotryptic digestion (10) and further modified by reaction with *N*-ethylmaleimide (11). Tetramethylrhodamine-5-iodoacetamide was purchased by Molecular Probes Europe BV, Leiden, The Netherlands. The compound was dissolved in dimethylformamide to prepare 6 mM stock solutions.

Protein sedimentation was performed in the Beckman TL100 rotor of the Beckman TL100 centrifuge for 10 min at 360000g. Total protein and protein in the supernatant solutions were measured either by the method of Bradford (12) or according to Lowry et al. (13).

**Preparation of the Fluorescent Actin Filaments.** To prepare fluorescent actin filaments F-actin was first coupled with tetramethylrhodamine-5-iodoacetamide. 2-Mercaptoethanol was removed from the F-actin solution by dialysis at 2 °C against a solution containing 5 mM bicarbonate, 5 mM

<sup>†</sup> This work was supported by grants of the University of Ferrara and of the Fondazione della Cassa di Risparmio di Ferrara.

\* Corresponding author: Enrico Grazi, Dipartimento di Biochimica e Biologia Molecolare, Università di Ferrara, Via Borsari 46, 44100 Ferrara, Italy. Phone 0039 0532 291421. Fax 0039 0532 202723. E-mail gre@ifeuniv.unife.it.

<sup>#</sup> Università di Ferrara.

<sup>‡</sup> Université de Bordeaux.

ascorbate, 2 mM  $\text{MgCl}_2$ , 0.1 M KCl, 0.2 mM ATP, and 2 mM  $\text{NaN}_3$ , pH 8.0. Tetramethylrhodamine-5-iodoacetamide (1 mol/per mol of actin) was then added to the F-actin (2 mg/mL) solution. After 17 h of incubation at 22 °C, the reaction was quenched by the addition of 5 mM 2-mercaptoethanol (final concentration) and diluted to 1 mg of actin/mL with the same buffer. The mixture was centrifuged for 10 min at 360000g in the TL100 rotor of the TL100 Beckman centrifuge. The fluorescent supernatant solution (0.75 mg of protein/mL) was supplemented with an equal amount (on molar basis) of G-actin and was allowed to copolymerize for 1 h at 22 °C in the presence of 100 mM KCl and 2 mM  $\text{MgCl}_2$  (final concentrations). Final concentration of actin was 1 mg/mL.

Immediately before the observation the fluorescent filaments were diluted to 20 nM (as actin monomer) in 16 mM phosphate, 3 mM  $\text{MgCl}_2$ , 1 mM  $\text{NaN}_3$ , and 1 mM 2-mercaptoethanol, pH 7.0. Under these conditions, the filaments survive the time needed for the observation (incidentally, under the same conditions critical concentration of pure actin is  $\sim 40$  nM).

**Coating Polystyrene Microspheres with *N*-Ethylmaleimide-Meromyosin.** Polystyrene microspheres (diameter 1  $\mu\text{m}$ , Polysciences Inc.) were washed in 0.1 M bicarbonate buffer, pH 9.6, resuspended, and washed three times in 20 mM phosphate buffer, pH 4.5. The microspheres (1 mL, 2.5% w/v) were then treated with a 1.2-mL solution (2% w/v) of 1-(3-dimethylaminopropyl)-3-ethyl carbodiimide hydrochloride in 20 mM phosphate buffer, pH 4.5. After 3–4 h of incubation, with stirring, microspheres were centrifuged, resuspended, and washed three times with 0.2 M borate buffer, pH 8.5. Microspheres were then coated with *N*-ethylmaleimide-meromyosin (1 mg/mL) by incubation for 20 min at 20 °C in 0.3 M KCl, 5 mM  $\text{MgCl}_2$ , 25 mM phosphate, pH 7.4.

**Construction of the Assay Cells.** Assay cells were constructed by assembling two glass cover slips in a recessed specimen holder. A cover slip surface was coated with *N*-ethylmaleimide-meromyosin treated microspheres by incubation for 15 min at 4 °C with the assay buffer (15 mM orthophosphate, 3 mM  $\text{MgCl}_2$ , 1 mM  $\text{NaN}_3$ , and 1 mM 2-mercaptoethanol, pH 7.0), treated for 20 min at 4 °C with a 1% solution of bovine serum albumin and rinsed twice with the assay buffer before the introduction in the holder. The cell was then filled with 0.2 mL of a solution containing 20 nM tetramethylrhodamine F-actin plus 0.05% (w/v) *N*-ethylmaleimide-meromyosin treated microspheres in the assay buffer. To minimize photobleaching an oxygen depletion system (4.5 mg/mL of glucose, 230  $\mu\text{g/mL}$  of glucose oxidase and 36  $\mu\text{g/mL}$  of catalase, final concentrations) was added to the solution in all the experiments. Finally, the second cover slip, also treated with bovine serum albumin, was placed over the holder.

**Microscopy and Laser Light Trap.** The holder was placed in the stage of an Olympus IX70 microscope equipped with a PLANAPO 100 X, N.A. 1.4 objective and a step motor driven x–y translation stage control (Luis Neuman, Goettingen, Germany). The vertical, z-axis, position was adjusted by changing the focus. The specimen cell was illuminated in bright field by a 100 W halogen lamp and in epifluorescence by a 75 W Xenon lamp. The images were captured by an Hamamatsu Newicon camera, recorded, and stored on a videotape. The single beam laser trap was generated

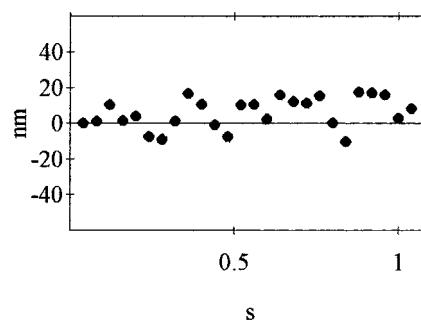


FIGURE 1: Displacement of the trapped microsphere because of the Brownian motion. Laser power was 50 mW. The distance from the focus on the x-axis was recorded at 40-ms time intervals.

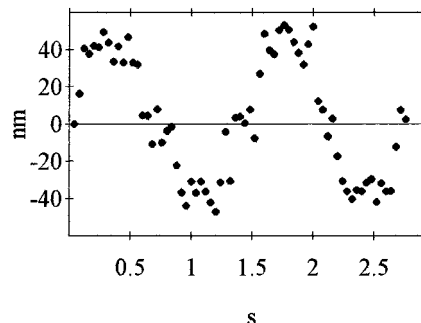


FIGURE 2: Displacement of the trapped microsphere because of the drag. Laser power was 50 mW. The distance from the focus on the x-axis was recorded at 40-ms intervals. The velocity of the stage along the x-axis was 30  $\mu\text{m/s}$ . The shift of the microsphere from the positive to the negative deviation from the focus was obtained by inverting the velocity of the stage.

by a Ti:Saph laser (Spectraphysics, Grenoble, France) pumped by a 2017S 6 W Argon laser (Spectraphysics, Grenoble, France). Experimental temperature (22 °C) was not significantly increased by the irradiation.

**Trap Stiffness Calibration.** The trapped microsphere undergoes Brownian motion. Evidence of this was obtained by recording at 40-ms intervals the displacement of the trapped microsphere along the x-axis (Figure 1).

The Stokes' force method was used to calibrate the force associated with the displacement of the microsphere from the center of the trap. A viscous drag, or Stokes', force was applied to a captured microsphere by moving the specimen holder along the x-axis in both versus (14, 15). This action promoted the displacement of the microsphere from the center of the trap. As it is shown in Figure 2, at the laser power of 50 mW and at the velocity of the stage of 30  $\mu\text{m/s}$ , the average displacement of the microsphere from the focus was 43.9 nm.

The Stokes force,  $F$  (dyne), on the microsphere was calculated by:

$$F = 6\pi\eta rv$$

where  $\eta$  (Poise) is the viscosity;  $r$  (cm) is the radius of the microsphere; and  $v$  ( $\text{cm s}^{-1}$ ) is the velocity of the displacement. When the velocity of the stage was increased from 13 to 125  $\mu\text{m s}^{-1}$ , the Stokes' force increased from 0.124 to 1.184 pN.

The linear relationship between microsphere displacement and Stokes' force was used to estimate the stiffness of the trap. Stiffness was found to increase by 0.0001957 pN  $\text{nm}^{-1}$  for the increase of 1 mW of the power of the trap (Figure

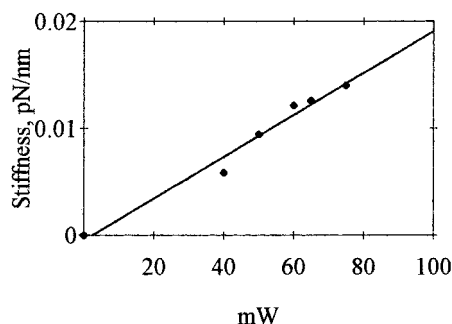


FIGURE 3: Relationship between stiffness and power of the trap. Data are fitted by the equation:  $\text{stiffness (pN nm}^{-1}\text{)} = -0.000456777 + 0.00019569 \text{ mW}$ .

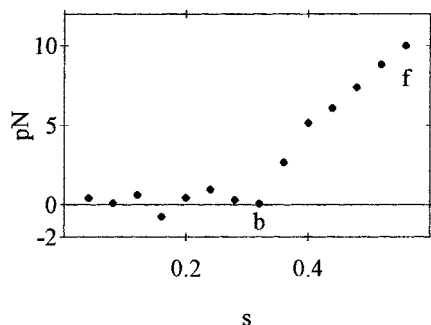


FIGURE 4: Stretching a S1-decorated actin filament. The actin filament was decorated with S1 at the 0.6:1 S1 to actin molar ratio. Power was 350 mW, and stiffness was  $0.0685 \text{ pN s}^{-1}$ . The distance from the focus on the  $x$ -axis was recorded at 40 ms intervals. At point b, the displacement of the stage was started. At point f, the filament broke.

3). The force on the microsphere at the trap was calculated as the product of the stiffness of the trap and the distance of the microsphere from trap center.

The system was usually operated at 300–400 mW. As an example, the stretching of a S1-decorated actin filament (0.6:1 S1 to actin molar ratio) is presented. Power was 350 mW, and stiffness was  $0.0685 \text{ pN s}^{-1}$ . The system was first observed at rest (0 – b), and then the displacement of the stage was started (b – f). The filament broke at point, f, when the applied force was 10 pN. Breaking was signaled by the sudden return of the microsphere at the center of the trap (Figure 4).

**Determination of the Length of the Filaments.** While the force applied to the filaments was estimated from the displacement of the trapped microsphere from the center of the trap, the length of the stretched filaments was detected directly by recording the position of both microspheres. Accordingly, one end of the actin filament was attached to a *N*-ethylmaleimide-meromyosin treated microsphere, suspended in the assay solution and trapped in the focus of the laser beam, and the other end of the filament was attached to a coated bead fixed to the lower coverslip. While the  $z$ -axis was focusing fixed, the microscope stage was moved either along the  $x$ - or the  $y$ -axis until the filament was broken. The process was followed both with the fluorescent and the bright field control. The stored bright field images of both the beads were analyzed by specific software.

The length of the filaments was calculated by the following formula:

$$\text{length (nm)} = \sqrt{(x_C - x_F)^2 (y_C - y_F)^2 + z_F^2}$$

where  $x$ ,  $y$ , and  $z$  indicate the coordinates; the subscripts, C and F, indicate the microsphere at the lower coverslip and the microsphere at the focus. The coordinate,  $z$ , was kept constant at 6500 nm. Due to the noise of recording and video, effective resolution was about 15 nm.

Curve fitting was performed by the “Mathematica” software.

## RESULTS

**Critical Concentration of Tetramethylrhodamine F-Actin.** Coupling with tetramethylrhodamine 5-iodoacetamide was found to disrupt the actin filament. However, the nonsedimentable products of the disruption were also found to copolymerize with G-actin, yielding fluorescent actin filaments.

To estimate the critical concentration of the copolymerized filaments is not easy since the fluorescent actin component does not sediment per se in polymerization buffers. To overcome this drawback, the copolymerized actin filaments suspension (equimolar amounts of G-actin and of the nonsedimentable fluorescent product) were diluted serially with the polymerization buffer (5 mM bicarbonate, 5 mM ascorbate, 2 mM  $\text{MgCl}_2$ , 0.1 M KCl, 0.2 mM ATP, and 2 mM  $\text{NaN}_3$ , pH 8.0), left 17 h at 22 °C, and centrifuged 10 min at 360000g. As expected, the protein concentration in the supernatant solutions decreased with the dilution of the sample, being 0.13, 0.09, 0.053, and 0.03 mg/mL, as compared to a total protein concentration of 0.5, 0.25, 0.125, and 0.062 mg/mL, respectively. The apparent critical concentration was  $\sim 0.03 \text{ mg/mL}$  or  $\sim 0.72 \text{ }\mu\text{M}$ . The same experiment was repeated with a copolymerized actin filaments suspension obtained by mixing G-actin and the nonsedimentable fluorescent product at the 0.7 to 0.3 molar ratio. The apparent critical concentration was  $\sim 0.029 \text{ mg/mL}$  or  $\sim 0.7 \text{ }\mu\text{M}$ . These values were close to that of pure F-actin under the same polymerizing conditions ( $0.013 \text{ mg/mL}$  or  $0.31 \text{ }\mu\text{M}$ ).

We refer here to an *apparent* critical concentration (a) because it is certainly overestimated due to the presence of the nonsedimentable, tetramethylrhodamine–actin oligomers and (b) because, in our opinion, G-actin is polymerizing on seeds of nonsedimentable tetramethylrhodamine–actin oligomers (6).

**Yield Strength of Tetramethylrhodamine F-Actin.** In all the experiments reported in this work, yield strength was measured on actin filaments obtained by copolymerizing G-actin with equimolar amounts (as the actin monomer) of the filament disruption products. These filaments are detected more easily than the filaments obtained at lower ratios of the nonsedimentable, tetramethylrhodamine–actin oligomers.

To measure the yield strength, one end of the actin filaments, free or decorated, was attached to a *N*-ethylmaleimide-meromyosin treated microsphere, suspended in the assay solution, and trapped in the focus of the laser beam, and the other end of the filament was attached to a coated bead fixed to the lower coverslip. While the  $z$ -axis was focusing fixed, the microscope stage was moved either along the  $x$ - or the  $y$ -axis until the filament was broken. Applied force was calculated from the displacement from the focus of the microsphere trapped by the laser beam.



Table 1: Yield Strength of Tetramethylrhodamine F-Actin<sup>a</sup>

filaments	$L_0$ , nm	$L_Y$ , nm	$(L_Y - L_0)/L_0$	yield strength, pN
1	8467	8901	0.051	3.9
2	7174	7537	0.0506	3.71
3	7599	7961	0.0476	3.31
4	7964	8331	0.046	3.56
5	7948	8275	0.041	3.73
6	7944	8285	0.043	3.66
7	7938	8308	0.0466	4.02
8	7644	7964	0.042	3.65
average $\pm$ sem			$0.046 \pm 0.0377$	$3.69 \pm 0.213$

<sup>a</sup> Resting length,  $L_0$ ; yield length,  $L_Y$ ; specific elongation at the yield point =  $(L_Y - L_0)/L_0$ .

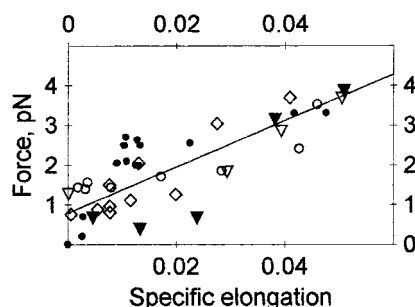


FIGURE 5: Force-specific elongation curves of tetramethylrhodamine F-actin filaments: 1 (▼); 2 (▽); 3 (●); 4 (○); 5 (◇). Specific elongation =  $(L - L_0)/L_0$ . Straight line: force (pN) =  $0.786537 + 58.123[\text{specific elongation}]$ .

Tetramethylrhodamine F-actin was diluted to 20 nM, as actin monomer, in 16 mM phosphate, 3 mM  $\text{MgCl}_2$ , 1 mM  $\text{NaN}_3$ , and 1 mM 2-mercaptoethanol, pH 7.0, plus the oxygen depletion system (see the methods section). Measurements were performed on eight filaments. The average specific elongation at the yield point,  $(L_Y - L_0)/L_0$ , was  $0.046 \pm 0.0377$ , where  $L_0$  is the rest length, and  $L_Y$  is the yield length. The yield strength was  $3.69 \pm 0.213$  pN (Table 1).

For five out of the eight filaments, the force-specific elongation curves were recorded and presented in Figure 5. Data were fitted quite reliably by the straight line:

$$\text{force (pN)} = 0.786537 + 58.123[\text{specific elongation}] \quad (1)$$

Data are more disperse at low than at high specific elongation, where they almost converge at the yield strength point. This is probably due to some uncertainty in the estimate of the actual rest length of the filaments ( $L_0$ ). This uncertainty may also explain why the straight line crosses the ordinate axis at a value different from zero.

**Effect of Tropomyosin on the Yield Strength of Tetramethylrhodamine F-Actin.** A solution was prepared containing 7  $\mu\text{M}$  tetramethylrhodamine F-actin and 1  $\mu\text{M}$  tropomyosin in 16 mM phosphate, 3 mM  $\text{MgCl}_2$ , 1 mM  $\text{NaN}_3$ , and 1 mM 2-mercaptoethanol, pH 7.0. After 60 min of incubation at 4 °C, the samples were diluted to 20 nM (as actin monomer) with the same buffer supplemented with the oxygen depletion system, and yield strength of the filaments was measured at 22 °C. Yield strength was found to increase from  $3.69 \pm 0.213$  pN, in the absence of tropomyosin (previous section), to  $10.51 \pm 0.24$  pN (average of six filaments) in the presence of tropomyosin. The values of the specific elongation at the yield point were quite disperse with the average value of

Table 2: Yield Strength of Tetramethylrhodamine F-Actin Decorated with Tropomyosin<sup>a</sup>

filaments	$L_0$ , nm	$L_Y$ , nm	$(L_Y - L_0)/L_0$	yield strength, pN
1	6588	6611	0.00349	10.41
2	6666	6712	0.0069	10.25
3	6663	6696	0.00495	10.8
4	6861	6876	0.00215	10.3
5	6580	6595	0.00228	10.5
6	6677	6710	0.00494	10.8
average $\pm$ SEM			$0.00408 \pm 0.0018$	$10.51 \pm 0.24$

<sup>a</sup> Resting length,  $L_0$ ; yield length,  $L_Y$ ; specific elongation at the yield point =  $(L_Y - L_0)/L_0$ .

Table 3: Tropomyosin-Decorated Tetramethylrhodamine F-Actin: Regression Lines of the Force-Specific Elongation Curves<sup>a</sup>

filaments	force, pN
1	$F = 0.28 + 2958s'$
2	$F = 0.54 + 1460s'$
3	$F = 1.46 + 1575s'$
4	$F = 4780s'$
5	$F = 0.25 + 4055s'$
6	$F = 0.125 + 2184s'$

<sup>a</sup>  $s' = (L - L_0)/L_0$ .

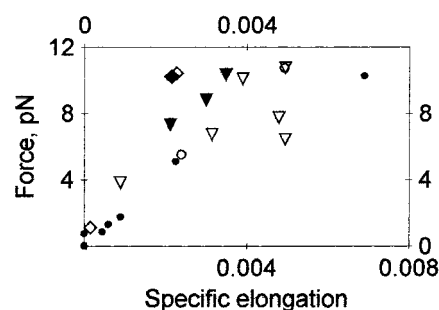


FIGURE 6: Force-specific elongation curves of tropomyosin-decorated tetramethylrhodamine F-actin filaments: 1 (▼); 2 (●); 3 (▽); 4 (◆); 5 (◇); 6 (○). Specific elongation =  $(L - L_0)/L_0$ .

$0.00408 \pm 0.0018$  (Table 2). Accordingly, the angular coefficients of the straight lines representing the data ranged from 1460 to 4780 (Table 3, Figure 6), thus indicating a significantly different behavior of the six filaments, perhaps due to inhomogeneous decoration by tropomyosin.

**Effect of Myosin Subfragment 1 on the Yield Strength of Tetramethylrhodamine F-Actin.** The incubation mixtures contained 1  $\mu\text{M}$  tetramethylrhodamine F-actin in 16 mM phosphate, 3 mM  $\text{MgCl}_2$ , pH 7.0, and were supplemented with either 0 or 0.2 or 0.4 or 0.6 or 0.8 or 1.0  $\mu\text{M}$  myosin subfragment 1. After 30–60 min of incubation at 4 °C, the samples were diluted to 20 nM (as actin monomer) with the same buffer and yield strength of the filaments was measured at 22 °C as described in the methods section.

As shown in Table 4 and in Figure 7, the addition of myosin subfragment 1 to tetramethylrhodamine F-actin, at the 0.2:1 molar ratio, displays a modest effect on the yield strength of the actin filament. The effect becomes progressively more significant at the higher ratios, up to a yield strength of  $15.81 \pm 0.26$  pN at the 1:1 molar ratio.

At this same ratio, the average specific elongation at the yield point is  $0.01 \pm 0.005$ .

The force-specific elongation curves of the six filaments (Figure 8) are satisfactorily represented by straight lines

Table 4: Effect of Myosin Subfragment S1 on the Yield Strength of Tetramethylrhodamine F-Actin<sup>a</sup>

S1/TMRF	$(L_Y - L_0)/L_0$	yield strength, pN
0.0 (8)	0.046	3.69
0.2 (4)	0.024	4.39
0.4 (5)	0.019	7.13
0.6 (4)	0.0053	9.58
0.8 (3)	0.0062	10.73
1.0 (6)	0.01	15.81

<sup>a</sup> S1/TMRF = S1 to tetramethylrhodamine F-actin molar ratio. Specific elongation at the yield point =  $(L_Y - L_0)/L_0$ . Numbers in parentheses indicate the number of filaments analyzed in each single experiment.

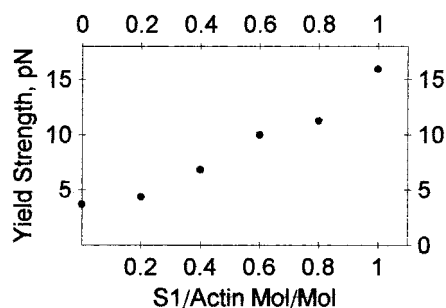
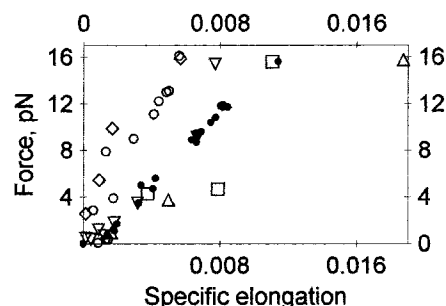


FIGURE 7: Yield strength of tetramethylrhodamine F-actin as a function of the S1 to actin ratio.

FIGURE 8: Force—specific elongation curves of myosin subfragment 1 decorated tetramethylrhodamine filaments: 1 ( $\Delta$ ); 2 ( $\square$ ); 3 ( $\circ$ ); 4 ( $\bullet$ ); 5 ( $\nabla$ ); 6 ( $\diamond$ ). Specific elongation =  $(L - L_0)/L_0$ .Table 5: S1-Decorated Tetramethylrhodamine F-Actin (1:1 Molar Ratio): Regression Lines of the Force—Specific Elongation Curves<sup>a</sup>

filaments	force, pN
1	$F = -0.216 + 856s'$
2	$F = -0.84 + 1243s'$
3	$F = 0.77 + 2530s'$
4	$F = -0.9 + 1511s'$
5	$F = -0.64 + 1773s'$
6	$F = 2.55 + 2550s'$

<sup>a</sup>  $s' = (L - L_0)/L_0$ .

(Table 5). The angular coefficients of these straight lines spans from 856 to 2550, thus indicating a significantly different behavior of the six filaments.

*Effect of the Decoration with Both Tropomyosin and Myosin Subfragment 1 (1:1 Actin to Myosin Molar Ratio) on the Yield Strength of Tetramethylrhodamine F-Actin.* A solution was prepared containing 1.4  $\mu$ M tetramethylrhodamine F-actin, 0.2  $\mu$ M tropomyosin and 1.4  $\mu$ M myosin subfragment 1 in 16 mM phosphate, 3 mM  $MgCl_2$ , 1 mM  $NaN_3$ , and 1 mM 2-mercaptoethanol, pH 7.0. After 60 min of incubation at 4  $^{\circ}C$ , the samples were diluted to 20 nM (as actin monomer) with the same buffer supplemented with

the oxygen depletion system, and yield strength of the filaments was measured at 22  $^{\circ}C$ . Yield strength of the decorated filaments was found to be  $22.3 \pm 0.48$  pN (average of eight filaments).

*The Elastic Modulus by Stretching of Tetramethylrhodamine F-Actin and of Its Derivatives Decorated either with Tropomyosin or with Myosin Subfragment-1.* The elastic modulus by stretching ( $M$ ) was calculated according to the equation:

$$M = \frac{1}{\pi r^2} \frac{dF}{ds'} \quad (2)$$

where  $r = 4.5$  nm is the radius of the actin filament (16),  $F$  is the force as a function of the specific elongation (Tables 3 and 5) and  $s' = (L - L_0)/L_0$  is the specific elongation. For uniformity, the same radius was taken for actin and for its derivatives.

The elastic modulus by stretching for tetramethyl rhodamine F-actin,  $M = 0.91$  MPa, is calculated by utilizing eq 1, which describes the average behavior of the five filaments examined.

The elastic modulus by stretching for tropomyosin-decorated tetramethyl rhodamine F-actin ranges between 23 MPa (filament 2, Table 3) and 75 MPa (filament 4, Table 3).

The elastic modulus by stretching for the 1:1 myosin subfragment 1—tetramethylrhodamine F-actin complex ranges between 13.45 MPa (filament 1, Table 5) and 40 MPa (filament 6, Table 5).

## DISCUSSION

The load on each single thin filament in the course of the isometric contraction of skeletal muscle can be estimated as follows. The average value of the isometric tension produced by a muscle fiber is  $245\,000\text{ N m}^{-2}$  with a maximum value of  $392\,000\text{ N m}^{-2}$  (17). If account is made for the portion of the section of the fiber occupied by nuclei, mitochondria, glycogen, etc., and the tension is referred to the section of the myofibrils only, it turns out that the actual tension is about 1.9 times larger than the tension measured on the whole fiber, and thus the average tension produced by the contractile apparatus is  $245000 \times 1.9 = 465000\text{ N m}^{-2}$  and the maximal tension is  $392000 \times 1.9 = 744800\text{ N m}^{-2}$  (18). The average force produced by a single myofibril (average radius 0.5  $\mu$ m, average section  $7.854 \times 10^{-13}\text{ m}^2$ ) ranges between the average value of 365 000 pN and the maximal value of 585 000 pN. Since in the isometric contraction of an intact fiber at the sarcomere length of 2.2  $\mu$ m, the center to center distance between the thick filaments is 46.2 nm (19), the area of the equilateral triangle defined by the centers of three thick filaments is  $7.854 \times 10^{-13}\text{ m}^2$ . The number of the thin filaments in the myofibril is given by the ratio between the section of the myofibril ( $7.854 \times 10^{-13}\text{ m}^2$ ) and the area of the triangle ( $9.24 \times 10^{-16}\text{ m}^2$ ) and equals 850. The average load on each single thin filament is thus  $365000\text{ pN}/850 = 429\text{ pN}$ , and the maximal load is  $585000\text{ pN}/850 = 688\text{ pN}$ .

Tetramethylrhodamine F-actin displays an apparent critical concentration of 0.72  $\mu$ M and bears a load of only 3.69 pN. Even assuming that pure actin (critical concentration 0.32  $\mu$ M) may bear 2–3 times larger loads, its yield strength still

remains about 2 orders of magnitude lower than that required for skeletal muscle contraction.

Decoration of tetramethylrhodamine F-actin with tropomyosin from skeletal muscle increases the yield strength of the filament by  $\sim 3$ -fold, from 3.69 to 10.51 pN. The increase is significant but still inadequate to support the function of the actin filament. Incidentally, Kishino and Yanagida (1), when testing phalloidin F-actin and the phalloidin F-actin tropomyosin complex, found comparable yield strengths for the two species. The difference is, on the contrary, very evident in our experiments, where F-actin is not labeled with phalloidin. Thus, phalloidin seems to swamp out the regulation by the ancillary proteins.

Decoration of tetramethylrhodamine F-actin with myosin subfragment-1 increases the yield strength of the filament by  $\sim 4$ -fold, from 3.69 to 15.81 pN, at the 1:1 S1 to actin molar ratio.

Decoration of tetramethylrhodamine F-actin with both tropomyosin and with myosin subfragment-1 (1 to 1 S1 to actin molar ratio) further increases the yield strength of the actin filament to 22.3 pN.

Both the decoration with tropomyosin and with myosin subfragment-1 display important effects on the elastic modulus by stretching of tetramethylrhodamine F-actin, which increases from 0.91 to 23–75 MPa after the decoration with tropomyosin and to 13–40 MPa after the decoration with myosin subfragment-1. These effects on the elastic modulus by stretching, particularly those promoted by myosin subfragment-1, could be of importance in the mechanics of muscle contraction since they indicate that the compliance of the actin filament changes as a function of cross-bridge attachment.

It is clear that decoration with either tropomyosin or with myosin subfragment-1 strengthens significantly the structure of the actin filament. It is also evident, however, that these decorated filaments are still inadequate for muscle contraction.

Adequacy of thin filament to muscle contraction is not a popular topic. Apparently, one is satisfied with the unnatural derivative phalloidin F-actin. We disagree on this. In our

opinion, a plausible mechanism of muscle contraction must rely on the knowledge of the mechanic properties of the natural thin filament and of the reasons why in vivo thin filament supports high loads. An important difference between the system we have studied in this work and the in vivo one is that in vivo the pointed end of the thin filament is capped and the barbed end is embedded in the Z disk. Capping both ends certainly stabilizes thin filament. In the near future, we thus intend to study the effect of capping on the yield strength of F-actin.

## REFERENCES

1. Kishino, A., and Yanagida, T. (1988) *Nature* 334, 74–78.
2. Kojima, H., Ishijima, A., and Yanagida, T. (1994) *Proc. Natl. Acad. Sci.* 91, 12962–12966.
3. Tsuda, Y., Yasutake, H., Ishino, A., and Yanagida, T. (1996) *Proc. Natl. Acad. Sci. U. S.* 93, 12937–12942.
4. Swartz, D. R. (1999) *J. Muscle Res. Cell Motil.* 20, 457–467.
5. Adami, R., Choquet, D., and Grazi, E. (1999) *Eur. J. Biochem.* 263, 1–7.
6. Cintio, O., Adami, R., Choquet, D., and Grazi, E. (2001) *Biophys. Chem.* 92, 201–207.
7. Pardee, J. D., and Spudich, J. A. (1982) *Methods Enzymol.* 85, 164–181.
8. Margossian, S. A., and Lowey, S. (1982) *Methods Enzymol.* 85, 55–71.
9. Smillie, L. B. (1982) *Methods Enzymol.* 85, 234–241.
10. Weeds, A. G. (1975) *Nature* 257, 54–56.
11. Reisler, E. (1982) *Methods Enzymol.* 85, 84–93.
12. Bradford, M. M. *Anal. Biochem.* 72, 248–254.
13. Lowry, O. H., Rosebrough, N. J., Farr A. L., and Randall R. J. (1951) *J. Biol. Chem.* 193, 265–275.
14. Harada, G., Sakurada, K., Aokoi, T., Thomas, D. D., and Yanagida, T. (1990) *J. Mol. Biol.* 216, 49–68.
15. Ashin, A. (1992) *Biophys. J.* 61, 569–582.
16. Holmes, K. C., Popp, D., Gebhard, D., and Kabsch, W. (1990) *Nature* 347, 44–49.
17. Edman, K. A. P. (1988) *J. Physiol. (London)* 404, 301–321.
18. Merah, Z. A., and Morel, J. E. (1993) *J. Muscle Res. Cell Motil.* 14, 552–553.
19. Haselgrove, J. C., and Huxley, H. E. (1973) *J. Mol. Biol.* 77, 549–568.

BI0116745